Published in final edited form as:
Cell Stem Cell. 2008 July 3; 3(1): 33–43. doi:10.1016/j.stem.2008.05.009.

Hair Follicle Stem Cells are Specified and Function in Early Skin Morphogenesis

Jonathan A. Nowak, **Lisa Polak**, **H. Amalia Pasolli**, and **Elaine Fuchs***
Howard Hughes Medical Institute Laboratory of Mammalian Cell Biology & Development The Rockefeller University New York, NY 10065

SUMMARY

In adult skin, epithelial hair follicle stem cells (SCs) reside in a quiescent niche and are essential for cyclic bouts of hair growth. Niche architecture becomes pronounced postnatally at the start of the first hair cycle. Whether SCs exist or function earlier is unknown. Here we show that quiescent cells appear early in skin development, express SC markers, and later give rise to the adult SC population. To test whether early quiescent cells function as SCs, we use *Sox9-Cre* for genetic marking and *K14-Cre* to embryonically ablate *Sox9*, an essential adult SC gene. We find that the progeny of Sox9-expressing cells contribute to all skin epithelial lineages and Sox9 is required for SC specification. In the absence of early SCs, hair follicle and sebaceous gland morphogenesis is blocked and epidermal wound repair is compromised. These findings establish the existence of early hair follicle SCs and reveal their physiological importance in tissue morphogenesis.

Keywords

stem cell niche; embryogenesis; skin; hair follicles; bulge; Sox9

INTRODUCTION

Adult stem cells (SCs) maintain tissues during normal homeostasis and wound repair. SCs frequently reside in specific niches which provide the appropriate microenvironment and molecular cues to preserve proliferative and tissue regenerative potential, the hallmarks of SCs (Blanpain and Fuchs, 2006; Moore and Lemischka, 2006). In mammalian hair follicles (HFs), SCs reside in a relatively quiescent state within a permanent, anatomically distinct region of the follicle known as the bulge. In adult mice, bulge SCs can contribute to all three epithelial lineages of skin (Blanpain et al., 2004; Morris et al., 2004; Oshima et al., 2001). During normal homeostasis, bulge SCs are periodically activated to fuel postnatal hair cycles. While the interfollicular epidermis (IFE) and sebaceous gland (SG) both contain resident populations of unipotent progenitor cells, multipotent bulge SCs can provide a cellular input to both of these lineages in a wound environment.

*To whom correspondence should be addressed Howard Hughes Medical Institute The Rockefeller University 1230 York Avenue, Box 300 New York, NY 10021 fuchs@rockefeller.edu Tel #212-327-7953 Fax #212-327-7954.

While all HFs have initiated development by P0 when mice are born, bulge niche architecture is not pronounced until three weeks after birth (~P20-P21) when mice already have a full hair coat (Cotsarelis, 2006; Schmidt-Ullrich and Paus, 2005). The distinctive appearance of the bulge at this age coincides with the onset of the growth phase (anagen) of the first postnatal hair cycle. Where the adult bulge SCs come from and how they organize within a niche remains unknown. It has been widely assumed that bulge SCs are not needed for embryonic morphogenesis, where HFs develop from epidermis rather than the base of preexisting bulge niches. In support of this notion, two widely used bulge SC markers, CD34 and a *keratin 15-LacZ* reporter gene, are both upregulated at ~P20 (Blanpain et al., 2004; Liu et al., 2003; Trempus et al., 2003). Additionally, while many studies using postnatal nucleotide tracer pulse-chase experiments have demonstrated the quiescence of adult bulge SCs (Cotsarelis et al., 1990; Morris and Potten, 1999; Taylor et al., 2000), the existence of a quiescent cell population within developing HFs has never been reported.

The isolation and transcriptional profiling of bulge SCs has revealed many new markers that offer additional insights into the characteristics and behavior of follicle SCs. Among the upregulated bulge genes are transcription factors Lhx2, Sox9, Tcf3 and Nfatc1 (Blanpain et al., 2004; Morris et al., 2004; Trempus et al., 2003; Tumbar et al., 2004). Interestingly and in contrast to CD34, their expression begins early in HF morphogenesis, with Lhx2 and Sox9 appearing at the placode stage and Tcf3 and Nfatc1 appearing later during the peg stage (Horsley et al., 2008; Nguyen et al., 2006; Rhee et al., 2006; Vidal et al., 2005). While null mutations in all four genes cause embryonic lethality, skin grafts from *Lhx2* and *Nfatc1* null embryos develop HFs which contain functional SC niches but display reduced SC quiescence (Horsley et al., 2008; Rhee et al., 2006). *Y10:Cre/Sox9(fl/fl)* mice target *Sox9* ablation to postnatal skin, revealing hair cycle defects that include a failure of adult bulge SCs to form and/or express CD34 (Vidal et al., 2005).

Despite the importance of these adult follicle SC transcription factors and their expression in embryonic skin, it is not known whether these genes function during morphogenesis. It is similarly unclear how and when the SC niche is established, an issue that is poorly understood for most tissues harboring stem cells. In this report, we use a combination of genetics, cell biology and *in vivo* functional assays to investigate the specification and initial function of epithelial SCs in the hair follicle. We find that these SCs are specified during the earliest stages of HF morphogenesis and that initial SC specification critically depends on Sox9. Furthermore, we find that early SCs can contribute to all three skin epithelial lineages and in their absence, the normal morphogenesis of HFs and SGs is blocked and epidermal wound repair is severely compromised.

RESULTS

Quiescent Bulge Cells are Specified in the Earliest Stages of Hair Follicle Morphogenesis

In order to determine when the quiescent bulge SC population is first specified, we modified *in vivo* pulse-chase experiments previously employed for labeling adult bulge cells with histone H2B-GFP (Tumbar et al., 2004). Similar to our previous strategy, we used *K5-Tet*^{off} mice to control keratin 5 (K5)-positive skin epithelial expression of histone H2B-GFP driven by a tetracycline regulatable enhancer, but in this case, we began our chase at embryonic day 18.5 (E18.5). At this early time, most hair follicles have been specified, but are still in the early stages of morphogenesis.

In unchased embryos, all skin epithelial cells displayed H2B-GFP epifluorescence, consistent with strong *K5 promoter* activity by E13.5 (Fig. 1A). After 3d of chase (P2), the brightest H2B-GFP cells in the epidermis were in non-proliferative suprabasal layers, as expected from the upward mode of terminal differentiation in this tissue. Surprisingly, the

brightest cells in the hair follicle were concentrated in a relatively narrow zone (bracketed) of outer root sheath (ORS). After 9d of chase when HF downgrowth was nearly complete (P8), H2B-GFP label retaining cells (LRCs) clustered prominently within this upper ORS zone. Marking completion of the pilosebaceous unit (Schmidt-Ullrich and Paus, 2005), SGs had emerged just above these LRCs (Fig. 1A).

Consistent with their relatively slow-cycling nature, these early follicle LRCs were largely negative for proliferative nuclear protein Ki67, which instead marked many cells located both above (infundibulum) and below (matrix) this zone (Fig. 1A). In mature follicles, a thin trail of H2B-GFP-positive cells (arrowheads) extended down the ORS from the concentrated LRC zone towards the hair bulb, which contains the highly proliferative, transit-amplifying population of matrix cells responsible for hair production. Intriguingly, some of the cells within this trail displayed decreased nuclear epifluorescence intensity and some were also negative for Ki67, suggestive of a potential precursor-product relation between brighter H2B-GFP LRCS in the upper ORS and dimmer H2B-GFP cells in the lower ORS.

Use of fluorescence activated cell sorting (FACS) to quantify label retention in keratinocytes from fractionated epidermis or HFs (dermis) revealed that unchased HF keratinocytes expressed relatively uniform amounts of label at E18.5 but after 3d of chase, the spectrum of GFP fluorescence had broadened, indicating that most HF keratinocytes had divided several times (Figure S1A). Over 4d of chase, the HF GFP spectrum continued to broaden and diminish in intensity, reflecting rapid cell divisions. That said, a clear tail of GFP-high cells persisted, indicative of a less proliferative subset of HF cells. The variable rates of HF cell division contrasted starkly with the more uniform epidermal cell division rates reflected by symmetric distributions of label retention (Figure S1A).

To determine whether early LRCs might be related to adult follicle SCs, we conducted immunofluorescence microscopy with antibodies against a number of adult bulge markers and compared their localization patterns with H2B-GFP (Fig. 1B). Consistent with prior reports (Nguyen et al., 2006;Vidal et al., 2005), transcription factors Tcf3 and Sox9 were expressed in P8 ORS. While not restricted to H2B-GFP LRCs, Tcf3 and Sox9 positive cells included the LRC zone (brackets). Notably, Nfatc1 and Lhx2 were also expressed in the LRC zone and displayed even greater restriction than Tcf3 and Sox9 (arrowheads). Whether embryonic or adult, the only other place where Nfatc1, Lhx2 and LRCs are known to co-localize is in adult bulge SCs (Horsley et al., 2008;Rhee et al., 2006;Tumbar et al., 2004).

To directly evaluate the relation between early follicle LRCs and adult bulge SCs, we labeled mice until E18.5 and then chased until P21, when the first postnatal hair cycle is initiated (Blanpain et al., 2004). After an entire cycle of hair growth, LRCs marked by H2B-GFP during embryogenesis were still present at P21 where they localized to the CD34-positive adult bulge SC niche and secondary hair germ (HG) (Figure 1C). This result, confirmed by FACS analysis on 22d chased mice (Figure S1B), established that the early LRC population present in chased P3 and P9 follicles is the major contributor to the adult bulge SCs that appear at P20-21.

Taken together, these results demonstrate that a quiescent population of cells is specified early in HF development, that LRCs localize to a specific region of the growing HF where they express many SC markers, and that early LRCs persist to form the adult bulge. Notably, all of these quiescent, presumptive bulge cells lost some label during a 22d chase that covered the first complete hair cycle, leading us to postulate that these cells play an active role in HF morphogenesis before being called upon to drive the periodic growth of the adult hair cycle.

Sox9 Marks a Subset of Placode Cells at the First Stage of HF Morphogenesis and Sox9-expressing Cells can Contribute to All Skin Epithelial Lineages

To determine whether early LRCs might be important for HF morphogenesis, we traced expression of the known SC markers that we found to co-localize with these cells. Of the four bulge transcription factors, only Lhx2 and Sox9 were known to be expressed in the early hair placodes (Rhee et al., 2006; Vidal et al., 2005). We focused on Sox9 as a particularly good candidate for regulating LRC establishment during embryogenesis, since fortuitous postnatal HF targeting of *Sox9(fl/fl)* mice with a *Y10:Cre* transgene had resulted in adult HFs that lacked CD34 and which could not be maintained (Vidal et al., 2005).

In WT E14.5 embryos, the skin was marked by uniform E-cadherin expression and Sox9 protein was not present (Figure 2A). As predicted from the pattern of *Sox9 in situ* hybridization (Vidal et al., 2005), Sox9 protein marked developing placodes as soon as they could be architecturally discerned in the main waves of HF specification (E15.5-P0). Interestingly and unexpectedly, however, nuclear Sox9 protein resided in the suprabasal cells of the placode rather than in the P-cadherin and Lhx2 positive basal layer (Figure 2B). No previous studies on genes or signaling pathways have uncovered the existence of this unique Sox9-positive cell population within the placode.

By the peg stage, Sox9-expressing cells concentrated in a region in the upper ORS with moderate P-cadherin expression, while the brightest PCad-positive cells localized to the leading edge of developing follicles (Figure 1C). Once sebaceous glands (SG) emerged, it was clear that this Sox9-expressing ORS zone encompassed the presumptive bulge region (Figure 2D). By P2, a trail of Sox9-positive cells extended down the ORS, diminishing towards the matrix which was negative for Sox9. As previously reported (Vidal et al., 2005), the bulge SCs of adult HFs were positive for Sox9 (Figure 2E). Real time PCR on FACS-purified skin cells revealed background levels of *Sox9* mRNA expression in all populations besides ORS, validating the accuracy of our Sox9 immunofluorescence results (Figure 2F).

Given the similarity between Sox9 expression and LRC location in developing HFs, we wondered whether Sox9-expressing cells in embryonic skin might actively contribute to HF morphogenesis. To test this possibility, we conducted a genetic marking analysis using *Sox9-Cre*/*R26R* skin. In this assay, *Sox9-Cre* expressing cells become permanently marked for *LacZ* expression, and all progeny of *Sox9-Cre* expressing cells can then be readily monitored over time by β-galactosidase cleavage of XGal to generate a blue dye.

Although some portions of backskin express *Sox9-Cre* as early as E10.5 (Akiyama et al., 2005), tailskin, which is similar to backskin (Braun et al., 2003), was free of *Sox9-Cre* activity prior to HF development. At E18.5, tailskin XGal reactivity paralleled Sox9 immunolabeling, specifically marking cells in the upper portion of developing HFs, but remaining absent from the leading edge of HFs and the IFE (Figure 2G). By P8, however, HFs were almost entirely blue, demonstrating that the population of Sox9-expressing cells in the upper ORS had contributed not only to all differentiated layers of the growing HF but also the SG. By the first telogen (P21), Sox9-derived progeny encompassed most if not all cells of the HF, including those of the infundibulum, SG, bulge and secondary hair germ, but were absent from IFE (Figure 2G).

In normal homeostasis, a resident unipotent progenitor population within the IFE maintains skin turnover. In response to wounding, however, adult bulge SCs can be recruited to the IFE to assist in repair (Ito et al., 2005; Claudinot et al., 2005; Levy et al., 2007). Interestingly in P3 *Sox9-Cre*/*R26R* mice, scratch wounding resulted in a robust contribution of *Sox9-Cre* marked HF cells into the regenerating IFE (Figure 2G). Taken together, these studies revealed that Sox9-expressing cells within developing skin display key properties of

adult HF stem cells in that they contribute to HF and SG morphogenesis and can repair an injured IFE.

Sox9 is Required for the Specification of Early Bulge Cells and Maintenance of their Characteristics

In conditionally targeted *Y10:Cre/Sox9(fl/fl)* mice, HFs produced an atrophic hair coat that was retained into adulthood, thereby directing that study to a role for Sox9 in the adult hair cycle (Vidal et al., 2005). In light of our finding that a Sox9-marked bulge may form during skin embryogenesis, however, we were intrigued that hair defects had been noted in *Y10:Cre Sox9* mice as early as P8 (Vidal et al., 2005). To directly test whether Sox9 is functionally required for skin morphogenesis, we targeted *Sox9* ablation using *K14-Cre*, active in skin by E13.5. At E16.5, when many follicles are present only as placodes, the *Sox9* locus had been efficiently targeted (Figures S2, 3A). At birth, *K14-Cre/Sox9(fl/fl)* (cKO) mice were phenotypically distinguished from WT by an 80% reduction in whisker number, and at P6, when the hair coat first appears, cKO mice displayed a smooth epidermal surface with no sign of protruding hairs. As cKO mice aged, they remained completely devoid of a hair coat (Figure S2). These findings strongly supported an early role for Sox9.

The effects of *Sox9* ablation during embryogenesis appeared to be specific for the early SC population in the presumptive bulge. Thus, despite a morphologically intact, K17-positive ORS, the thickening that normally marks the location of early Sox9-positive bulge cells was missing (Figures S3A, 3B). Moreover, in contrast to WT HFs, where nuclear Nfatc1 marked a few cells within the presumptive bulge, Nfatc1 was never detected in developing cKO skin (Figure 3C, S3B). Additionally, even though Sox9 was absent in cKO hair germs, Lhx2 was still expressed initially in its normal location at the leading edge; however, Lhx2 failed to appear subsequently in the presumptive bulge (Figure 3D). Finally, although Tcf3 was detected initially in the ORS of developing cKO follicles, it was progressively lost during the first week after birth (Figure 3E). Notably, the earliest disappearance of Tcf3 occurred within the presumptive bulge region, and then proceeded unidirectionally towards the follicle base (Figure 3E).

Although establishment of early bulge architecture and gene expression was clearly impaired in developing Sox9-deficient HFs, it remained possible that early bulge cells were still present within the ORS but could no longer be identified by these criteria. Since our studies had shown that early bulge cells reduce their cycling rate as they develop, we conducted an embryonic BrdU pulse-chase to see if early LRCs were also lost when Sox9 was absent. Strikingly, significant differences in the numbers of cKO follicles with LRCs were already evident by P2 and by P6, LRCs were diminished by ~8X fold (Figures 3F, S3C). The dramatic reduction in LRCs in the presumptive bulge of Sox9-deficient neonatal HFs was accompanied by a substantial increase in proliferation in this zone. A 6 hr pulse of BrdU at P6 revealed an increase of ~40% in BrdU-labeled cells within the total *Sox9* cKO upper ORS population, mostly concentrated in the region of the presumptive bulge (Figure 3G). Similar differences were observed with proliferation markers Ki67 and G1/S-regulatory kinase Cdk4 (Figure S3D-E).

Our findings unveiled new requirements for Sox9, namely in the early expression and maintenance of transcription factors and slow-cycling bulge SC features which we found to be established during embryogenesis, long before other bulge markers, such as CD34, appear. When taken together with our earlier label-retaining and genetic marking studies, these additional data provided compelling evidence that not only does a population of early bulge stem cells form during skin development, but that its features critically rely upon one of the transcription factors that marks it.

Early Bulge Cells are Required to Maintain a Transit-amplifying Population of Matrix Cells Needed to Complete HF Morphogenesis

We next addressed our finding that Sox9-dependent early bulge SCs form during HF morphogenesis in the context of the absent hair coat phenotype of *Sox9* cKO mice. Histological analysis of skin from our P0 cKO mice revealed no significant differences in overall HF density or developmental stage (Figures 4A, S4A). By contrast, differences in HF length were already evident at P0 and by P6, cKO follicles averaged ~60% the length of WT follicles (Figure 4A). Despite gross perturbations in HF length, overall morphology and biochemical features of HF differentiation were relatively normal, and the ORS, IRS and hair shaft all appeared to be present and correctly organized (Figure S4, B-H). Importantly, *K14-Cre* targeted *Sox9* ablation efficiently prior to the main waves of HF specification and well before differentiated HF lineages developed. Thus, rather than specifying HFs or governing their differentiation, Sox9 appeared to function in maintaining the growth of HFs once morphogenesis was initiated.

To investigate this fascinating possibility further, we returned to *Sox9-Cre/R26R* mice, this time focusing on the developmental activity of Sox9-expressing cells at the same time points when defects became apparent in *Sox9* cKO mice. At P0 and P2, blue cells were detected in the upper ORS (bracketed) (Figure 4B). Notably, the initial matrix was negative for XGal reactivity. By P4 however, a trail of blue cells extended from the ORS into the matrix (Figure 4B, arrowheads). By P7, most matrix cells were blue, and only small patches of negative cells could be detected within the hair bulb (asterisk). Since the matrix was negative for *Sox9* mRNA and protein, the progressive expansion of XGal reactivity into these compartments at the expense of unmarked cells implies that during early HF development, Sox9-expressing cells provide an active input to the newly formed matrix, whose initial residents are transient.

To test whether the loss of early bulge SCs in *Sox9* cKO mice might result in an early failure to maintain the transit-amplifying matrix population, we next analyzed matrix size over time. No differences were noted at P0, suggesting that initial specification of matrix was unimpaired in the absence of early SCs (Figure 4C). However, in contrast to WT matrix, which gradually expanded from P0 to P10, *Sox9* cKO matrix only transiently expanded until P2 before it began to shrink and nearly disappear by P10 (Figure 4C). Concomitant with the loss of Ki67-positive matrix cells was an abrupt change in dermal papilla morphology (Figure S5), commensurate with that known to occur upon exit of HFs from the growth phase of the hair cycle (Stenn and Paus, 2001). Moreover, *Sox9* cKO HFs failed to proceed through any further stages of the hair cycle at later timepoints, consistent with the requirement of HF SCs in driving hair cycle progression (data not shown) and with the absence of a hair coat in our mice.

Direct evidence for a decreased input of SCs to the matrix in *Sox9* cKO HFs was provided by a series of short BrdU pulse chase experiments which allowed us to distinguish possible causes of a smaller matrix population, including precocious differentiation, decreased proliferation or impaired input of SCs to the matrix. At all times, the percentage of BrdU-positive cells per bulb was similar, suggesting that cKO cells proliferate at the same rate as WT cells (Figures 4D, S6A). Additionally, only minor differences in differentiation rate were detected, suggesting that the relative balance of proliferation and differentiation was largely unimpaired (Figures 4D, S6A). The cKO HFs were also generally free of apoptotic cells, suggesting that cell death was not a major cause of smaller matrix size (Figure S7). Strikingly, however, cKO HFs displayed a marked decline in ORS input to the matrix, with an ~33% reduction in the percentage of BrdU-positive cells in the lower ORS at 12h and an ~50% reduction at 20h (Figures 4D, S6A).

Based upon these results, the initial cells that formed the matrix and differentiated HF lineages appeared to be transient and not dependent upon Sox9 for their formation. However, without the Sox9-positive early bulge SCs, this pool of transit amplifying matrix cells was not maintained and as a direct consequence, HFs did not progress through the growth phase of the hair cycle.

Early Bulge Cells are Required for Formation of the Sebaceous Lineage

Although SGs possess their own resident unipotent progenitors marked by Blimp1, adult bulge SCs can differentiate along a sebaceous lineage in a wound environment or when SG progenitors are defective (Blanpain et al., 2004; Horsley et al., 2006; Morris et al., 2004). Based upon our *Sox9-Cre* marking results and the temporal appearance of early bulge SCs prior to development of SGs, we wondered whether early bulge SCs might be essential for this lineage. Indeed, Blimp1-positive SG progenitors were absent in cKO follicles (Figure 5A). Also missing was PPARγ, a key sebocyte differentiation marker (Figure 5B). Lipid dye (Oil-red O), which normally permits visualization of SG morphology by P6 only stained the subcutaneous adipocytes and revealed no signs of SGs in cKO follicles (Figure 5C).

Early Bulge Cells are Required for Follicle-mediated Regeneration of the Interfollicular Epidermis in a Wound Environment

Our genetic marking experiments using *Sox9-Cre* mice also provided evidence that HF cells derived from a Sox9-expressing population can contribute to repair of wounded IFE. To test whether Sox9-expressing early bulge SCs might be essential for efficient HF contribution to IFE repair, we conducted engraftment experiments on *Nude* mouse recipients with split-thickness P0.5 dermis/HF tissue (Figure S8A). Pilot experiments with *K14-H2BGFP* mice validated the split thickness grafting technique, yielding >90% GFP-positive donor cell IFE reconstitution (Figures S8B, S8C). To distinguish donor from host cell contributions in our Sox9 test grafts, male skins were grafted onto female *Nude* recipients, and fluorescence *in situ* hybridizations were performed with a Y chromosome specific probe (Y-FISH).

The data from the engraftments of *Sox9* cKO vs WT skins are summarized in Figure 6. Full and split thickness grafts from WT mice displayed comparably thick, uniform hair coats, and quantification of skin surface areas revealed no significant differences. Similarly, although full thickness grafts from *Sox9* cKO skin lacked hair and showed a slightly scaly epidermis, the average graft areas were similar to WT. All of these grafts expanded in size over time, indicating their robust nature in growth and ability to repair wounds. Y-FISH revealed that the IFE of all of these grafts was almost completely donor-derived.

While split thickness grafts from cKO skin were initially the same size as the other grafts, they always shrank substantially within a 6 week period and displayed markedly reduced numbers (typically ~15%) of Y-positive IFE cells (Figures 6A,C). The presence of Y-positive dermal cells underlying the Y-negative IFE confirmed the efficacy of the initial grafting procedure, and a delay in IFE regeneration was ruled out by monitoring grafts for up to 16 wk after engraftment (Figures 6B,D), at which time the percentage of Y-positive IFE cells had further decreased. These experiments revealed that, despite their later acquisition of IFE markers (Figure S9), neonatal *Sox9* cKO HFs lacking early SCs are severely impaired in their ability to repair damaged IFE.

DISCUSSION

Since quiescence is a hallmark of cells residing in the adult bulge SC niche (Cotsarelis et al., 1990; Morris and Potten, 1999; Taylor et al., 2000), we reasoned that by determining when and where quiescence is established, we might use this property to identify and characterize

an early SC population within HFs and trace the development of adult SCs. Our embryonic pulse-chase studies demonstrated that HF LRCs are specified early in morphogenesis, and begin to accumulate in a specific region of the HF where they express bulge-preferred transcription factors. Although early expression of several of these markers has been noted previously, the physiological significance of their expression at this early time had not been realized nor was it known that their expression correlated with the emergence of a developing niche of LRCs. Our studies place these earlier clues in perspective and firmly establish the existence of a functional niche of multipotent, quiescent SCs within early developing HFs.

Importantly, by extending the chase after embryonic labeling, we demonstrated that early LRCs are the direct precursors of the LRCs that reside in the adult bulge niche. Interestingly, while early LRCs express many of the same transcription factors that adult bulge cells do, they do not express CD34, which has widely been used as a key SC marker (Trempus et al., 2003; Morris et al., 2004; Blanpain et al., 2004). While the physiological significance of CD34 remains unclear, Sox9 has emerged as a key regulator of stem cell identity, marking both early and adult SCs. Sox9 also marks the trail of follicle SCs that appear to migrate from the bulge to the transit amplifying matrix during the HF growth phase.

By taking advantage of Sox9 as a marker of early LRCs, we were able to trace the origins of early bulge SCs to the hair placode. It is intriguing that placodes consist of two populations of cells that can be distinguished by their differential expression of Lhx2 and Sox9, since these two markers are later co-expressed not only by early bulge SCs but also adult bulge SCs. Our *Sox9* genetic marking studies suggest that the early basal placode cells that are marked by Lhx2 and P-cadherin are transient. They give rise to the initial hair bulb, but then seem to disappear entirely by ~P7. By contrast, the Sox9-expressing cell population which starts as only a few cells within the suprabasal layer of the placode gives rise not only to the long-lived, self-renewing SCs of the bulge but also the entire pilosebaceous unit, including the infundibulum. Moreover, concomitant with the emergence of Sox9-positive early LRCs is the expression of Lhx2, Nfatc1 and Tcf3 which thereafter continue to identify the multipotent SCs of the HF.

In the adult follicle, the active, cycling portion is thought to originate from bulge SCs (Ito et al., 2004). How and why is a separate transit amplifying population specified during initial HF morphogenesis? While additional experiments will be necessary to fully elucidate the significance of this finding, it is interesting that a developmental paradigm of using separate TA and SC populations during morphogenesis has also been described in blood development, where hemogenic cells drive primitive hematopoiesis before long-term hematopoietic SCs commence definitive hematopoiesis (Orkin and Zon, 2008). Our studies now pave the way for examining expression patterns of other adult SC markers in these two placode residences and should allow us to predict how a given gene might function to control subsequent HF morphogenesis.

The existence of an initial pool of Sox9-independent matrix cells explains why HF morphogenesis and differentiation begin normally in *Sox9* cKO embryos. The premature exhaustion of these transient cells in the absence of subsequent input from Sox9-positive SCs further explains why HF maturation and hair production halt midstream during morphogenesis. These findings also demonstrate convincingly that the initial matrix relies upon input from early Sox9-positive SCs for its maturation, and that matrix cells cannot enhance their own self-renewal to compensate for a lack of early bulge SC input.

Some years ago, Oshima et al. (2001) observed that in the anagen phase of the adult rat whisker, bulge cells continue to migrate along the ORS to the hair follicle bulb, where they

become matrix cells. Since this initial report, it has been widely debated whether this phenomenon is merely another feature unique to whisker follicles or whether backskin bulge SCs posess similar activity. Our studies on the development of WT and Sox9-deficient backskin follicles not only provide compelling evidence in support of the Oshima studies, but also show that the fueling of the matrix by Sox9-positive bulge cells is functionally required to maintain the matrix.

Another surprising finding that emerged from targeting *Sox9* ablation in the embryo was that SGs failed to form, even though Sox9 was not expressed in the SG lineage or its resident progenitors. The dependency of the SG lineage on Sox9-expressing cells was particularly intriguing considering that the emergence of Sox9-marked LRCs occurred just before that of sebaceous glands. Taken together, the inability of HF morphogenesis to proceed without Sox9-positive cells and the failure of SGs to form altogether establishes the early Sox9-expressing population as a multipotent SC pool essential for completing skin morphogenesis. These important conclusions could not be predicted from postnatal ablation of *Sox9* in the skin (Vidal et al., 2005), and they provide major new insights into the existence and usage of a follicle stem cell population at a stage and for a purpose that has hitherto been unanticipated.

Although nucleotide double-labeling experiments have detected HF-derived contributions to the IFE of young neonatal mice (Taylor et al., 2000), lineage tracing studies with a *Shh-Cre* reporter active in the developing placode suggest that the development of HFs and IFE involves distinct progenitors (Levy et al., 2005). Our *Sox9-Cre* lineage tracing experiments are consistent with *Shh-Cre* studies in showing that *Sox9-Cre* marked cells in the HF do not contribute to IFE either during its development or its subsequent homeostasis. However, our studies further revealed that in a wound response, *Sox9-Cre* marked HF cells in neonatal mice were robustly recruited to repair the IFE. This finding underscored the similarities between early bulge SCs and adult bulge SCs aiding in IFE repair (Ito et al., 2005; Levy et al., 2005; Levy et al., 2007; Tumbar et al., 2004). Our split thickness grafting approach allowed us to further measure the IFE reconstitution efficiency of early bulge SCs in a wound response and in long-term wound repair. Not only did HF-derived progeny repopulate the IFE with close to 100% efficiency, but these cells were also maintained stably over a four month period. Moreover, HFs from *Sox9* cKO mice lacking early SCs were highly impaired in regenerating IFE, suggesting that early SCs may be essential in order for follicles to participate in this process.

Our model summarizing the roles of Sox9-dependent early SCs in skin morphogenesis is presented in Figure 7. We've found that a quiescent SC population is formed during the earliest stages of HF morphogenesis and subsequently gives rise to cells in the adult bulge SC niche. This early SC population is essential for normal morphogenesis of both HFs and SGs, and it robustly contributes to the IFE lineage in a wound environment. While we have identified a single gene, Sox9, which is required for early SC specification, our studies now set the foundation for identification of additional molecules and pathways involved in the formation and regulation of these early SCs. A comprehensive understanding of the embryonic origins of SC development is an essential first step not only for normal tissue biology but also for a wide variety of human diseases, including cancers, where SC and/or niche biology is genetically altered.

EXPERIMENTAL PROCEDURES

Mice and Labeling Experiments

K14-H2BGFP (Tumbar et al., 2004), *BATGal* (Maretto et al., 2003) and *pTRE-H2BGFP/K5-tetVP16* (Tumbar et al., 2004) mice have been described. *Sox9-IRES-Cre* mice (Akiyama

et al., 2005) were crossed to *ROSA26*$^{Flox\text{-}Stop\text{-}Flox\text{-}\beta geo}$ (*R26R)* mice (Mao et al., 1999). *Sox9*$^{flox/flox}$ mice (Akiyama et al., 2002) were crossed with *K14-Cre* mice (Vasioukhin et al., 1999).

For H2B-GFP pulse-chase experiments, pregnant *pTRE-H2BGFP/K5-tetVP16* females with known plug dates were fed continuously with doxycycline chow beginning at E18.5. 5-Bromo-2'-deoxyuridine (BrdU) embryonic pulse-chase experiments were conducted by injecting pregnant females carrying E17.5 embryos with an intraperitoneal (IP) loading dose of 50μg/g BrdU and adding BrdU to drinking water for a 24 hour period at 0.8mg/mL. Postnatal BrdU experiments were conducted by single IP injection of 50μg/g BrdU.

Engraftment Experiments

Full thickness grafts from newborn mice were performed as described (Rhee et al., 2006). For split thickness grafts, backskin from P0 mice was placed dermis-side down in 5mM EDTA in PBS for 1 hour at 37°C. The epidermis was then removed as a single sheet from HF/dermis, which was then grafted in the same manner as full thickness grafts. In all cases, paired WT and cKO tissues of identical size were grafted on a single *Nude* recipient. Bandages were removed 12-14 days after grafting. Graft area was measured using a Canon Powershot S70 camera attached to a dissecting microscope and quantified using ImageJ software and a calibrated standard area.

FACS Analysis

HF/dermis cells from P0.5-P6 mice were isolated as previously described (Rendl et al., 2005), and epidermal cells were isolated by brief trypsinization of the epidermal sheet removed from full thickness skin after overnight 4°C dispase treatment. Cell isolation from P21 mice and all FACS stainings were performed as previously described (Blanpain et al., 2004). FACS analyses were performed on a FACSCalibur flow cytometer (BD Biosciences) using CellQuest Pro software.

RNA Analysis

Epidermal cells were collected by trypsinization of either full thickness E16.5 skin, or dispase-separated epidermis from P0.5 and P4 skin. ORS, Mx, DP, DF and Mc populations were prepared as previously described (Rendl et al., 2005). Total RNA was isolated using the Absolutely RNA Kit (Stratagene) and cDNA was synthesized using SuperScript III (Invitrogen). RT-PCR was performed on a LightCycler 480 (Roche) using SYBR Green I master mix. Sox9 mRNA expression levels were expressed as a function of GADPH mRNA.

Histology

Skins were embedded in OCT, frozen, sectioned and fixed in 4% paraformaldehyde. Immunofluoresence, XGal staining, hematoxylin/eosin staining, and *in situ* hybridizations were performed on OCT sections as previously described (Kaufman et al., 2003). Alkaline phosphatase detection of DP and Oil-red O staining of SGs were performed on OCT sections as previously described (Horsley et al., 2006; Rendl et al., 2005). Y-FISH analysis was performed on OCT sections using a Cy3 Star*FISH detection kit (Cambio). For immunohistochemistry, skins were fixed in formaldehyde and then dehydrated and embedded in paraffin. Antigen unmasking was performed using a Retriever 2100 for 20 min (Pick Cell Laboratories BV). Detection of immunohistochemical staining was performed using a Vectastain ABC kit (Vector Laboratories). Student's t-test was used to determine statistical significance.

Supplementary Material

Refer to Web version on PubMed Central for supplementary material.

Acknowledgments

We especially thank Benoit de Crombrugghe (Baylor U) and Andreas Schedl (INSERM, Nice) for their generosity in providing us with *Sox9-Cre* and *Sox9(fl/fl)* mice, respectively. Mice were housed and bred in the LARC ALAAC-accredited animal facility at The Rockefeller University, and we are especially grateful to Nicole Stokes for her technical assistance related to the expert care of these mice. We also thank Danelle Devenport, Valerie Horsley and Rui Yi in the Fuchs' laboratory for their critical reading of this manuscript, and Horace Rhee for pilot studies on embryonic LRCs. JN is an MD/PhD student supported by NIH MSTP grant GM07739 and partially by NRSA training grant CA09673; EF is an Investigator of the Howard Hughes Medical Institute. This work was supported in part from a grant from the NIH (EF).

REFERENCES

Akiyama H, Chaboissier MC, Martin JF, Schedl A, de Crombrugghe B. The transcription factor Sox9 has essential roles in successive steps of the chondrocyte differentiation pathway and is required for expression of Sox5 and Sox6. Genes Dev 2002;16:2813–2828. [PubMed: 12414734]

Akiyama H, Kim JE, Nakashima K, Balmes G, Iwai N, Deng JM, Zhang Z, Martin JF, Behringer RR, Nakamura T, et al. Osteo-chondroprogenitor cells are derived from Sox9 expressing precursors. Proc Natl Acad Sci U S A 2005;102:14665–14670. [PubMed: 16203988]

Akiyama H, Lyons JP, Mori-Akiyama Y, Yang X, Zhang R, Zhang Z, Deng JM, Taketo MM, Nakamura T, Behringer RR, et al. Interactions between Sox9 and beta-catenin control chondrocyte differentiation. Genes Dev 2004;18:1072–1087. [PubMed: 15132997]

Blanpain C, Fuchs E. Epidermal stem cells of the skin. Annual review of cell and developmental biology 2006;22:339–373.

Blanpain C, Lowry WE, Geoghegan A, Polak L, Fuchs E. Self-renewal, multipotency, and the existence of two cell populations within an epithelial stem cell niche. Cell 2004;118:635–648. [PubMed: 15339667]

Braun KM, Niemann C, Jensen UB, Sundberg JP, Silva-Vargas V, Watt FM. Manipulation of stem cell proliferation and lineage commitment: visualisation of label-retaining cells in wholemounts of mouse epidermis. Development 2003;130:5241–5255. [PubMed: 12954714]

Cotsarelis G. Epithelial stem cells: a folliculocentric view. J Invest Dermatol 2006;126:1459–1468. [PubMed: 16778814]

Cotsarelis G, Sun TT, Lavker RM. Label-retaining cells reside in the bulge area of pilosebaceous unit: implications for follicular stem cells, hair cycle, and skin carcinogenesis. Cell 1990;61:1329–1337. [PubMed: 2364430]

Horsley V, Aliprantis AO, Polak L, Glimcher LH, Fuchs E. NFATc1 balances quiescence and proliferation of skin stem cells. Cell 2008;132:299–310. [PubMed: 18243104]

Horsley V, O'Carroll D, Tooze R, Ohinata Y, Saitou M, Obukhanych T, Nussenzweig M, Tarakhovsky A, Fuchs E. Blimp1 defines a progenitor population that governs cellular input to the sebaceous gland. Cell 2006;126:597–609. [PubMed: 16901790]

Ito M, Kizawa K, Hamada K, Cotsarelis G. Hair follicle stem cells in the lower bulge form the secondary germ, a biochemically distinct but functionally equivalent progenitor cell population, at the termination of catagen. Differentiation; research in biological diversity 2004;72:548–557.

Ito M, Liu Y, Yang Z, Nguyen J, Liang F, Morris RJ, Cotsarelis G. Stem cells in the hair follicle bulge contribute to wound repair but not to homeostasis of the epidermis. Nature medicine 2005;11:1351–1354.

Kaufman CK, Zhou P, Pasolli HA, Rendl M, Bolotin D, Lim KC, Dai X, Alegre ML, Fuchs E. GATA-3: an unexpected regulator of cell lineage determination in skin. Genes Dev 2003;17:2108–2122. [PubMed: 12923059]

Levy V, Lindon C, Harfe BD, Morgan BA. Distinct stem cell populations regenerate the follicle and interfollicular epidermis. Dev Cell 2005;9:855–861. [PubMed: 16326396]

Levy V, Lindon C, Zheng Y, Harfe BD, Morgan BA. Epidermal stem cells arise from the hair follicle after wounding. Faseb J 2007;21:1358–1366. [PubMed: 17255473]

Liu Y, Lyle S, Yang Z, Cotsarelis G. Keratin 15 promoter targets putative epithelial stem cells in the hair follicle bulge. J Invest Dermatol 2003;121:963–968. [PubMed: 14708593]

Mao X, Fujiwara Y, Orkin SH. Improved reporter strain for monitoring Cre recombinase-mediated DNA excisions in mice. Proc Natl Acad Sci U S A 1999;96:5037–5042. [PubMed: 10220414]

Maretto S, Cordenonsi M, Dupont S, Braghetta P, Broccoli V, Hassan AB, Volpin D, Bressan GM, Piccolo S. Mapping Wnt/beta-catenin signaling during mouse development and in colorectal tumors. Proc Natl Acad Sci U S A 2003;100:3299–3304. [PubMed: 12626757]

Moore KA, Lemischka IR. Stem cells and their niches. Science 2006;311:1880–1885. [PubMed: 16574858]

Morris RJ, Liu Y, Marles L, Yang Z, Trempus C, Li S, Lin JS, Sawicki JA, Cotsarelis G. Capturing and profiling adult hair follicle stem cells. Nat Biotechnol 2004;22:411–417. [PubMed: 15024388]

Morris RJ, Potten CS. Highly persistent label-retaining cells in the hair follicles of mice and their fate following induction of anagen. J Invest Dermatol 1999;112:470–475. [PubMed: 10201531]

Nguyen H, Rendl M, Fuchs E. Tcf3 governs stem cell features and represses cell fate determination in skin. Cell 2006;127:171–183. [PubMed: 17018284]

Orkin SH, Zon LI. Hematopoiesis: an evolving paradigm for stem cell biology. Cell 2008;132:631–644. [PubMed: 18295580]

Oshima H, Rochat A, Kedzia C, Kobayashi K, Barrandon Y. Morphogenesis and renewal of hair follicles from adult multipotent stem cells. Cell 2001;104:233–245. [PubMed: 11207364]

Rendl M, Lewis L, Fuchs E. Molecular dissection of mesenchymal-epithelial interactions in the hair follicle. PLoS Biol 2005;3:e331. [PubMed: 16162033]

Rhee H, Polak L, Fuchs E. Lhx2 maintains stem cell character in hair follicles. Science 2006;312:1946–1949. [PubMed: 16809539]

Schmidt-Ullrich R, Paus R. Molecular principles of hair follicle induction and morphogenesis. Bioessays 2005;27:247–261. [PubMed: 15714560]

Stenn KS, Paus R. Controls of hair follicle cycling. Physiol Rev 2001;81:449–494. [PubMed: 11152763]

Taylor G, Lehrer MS, Jensen PJ, Sun TT, Lavker RM. Involvement of follicular stem cells in forming not only the follicle but also the epidermis. Cell 2000;102:451–461. [PubMed: 10966107]

Trempus CS, Morris RJ, Bortner CD, Cotsarelis G, Faircloth RS, Reece JM, Tennant RW. Enrichment for living murine keratinocytes from the hair follicle bulge with the cell surface marker CD34. J Invest Dermatol 2003;120:501–511. [PubMed: 12648211]

Tumbar T, Guasch G, Greco V, Blanpain C, Lowry WE, Rendl M, Fuchs E. Defining the epithelial stem cell niche in skin. Science 2004;303:359–363. [PubMed: 14671312]

Vasioukhin V, Degenstein L, Wise B, Fuchs E. The magical touch: genome targeting in epidermal stem cells induced by tamoxifen application to mouse skin. Proc Natl Acad Sci U S A 1999;96:8551–8556. [PubMed: 10411913]

Vidal VP, Chaboissier MC, Lutzkendorf S, Cotsarelis G, Mill P, Hui CC, Ortonne N, Ortonne JP, Schedl A. Sox9 is essential for outer root sheath differentiation and the formation of the hair stem cell compartment. Curr Biol 2005;15:1340–1351. [PubMed: 16085486]

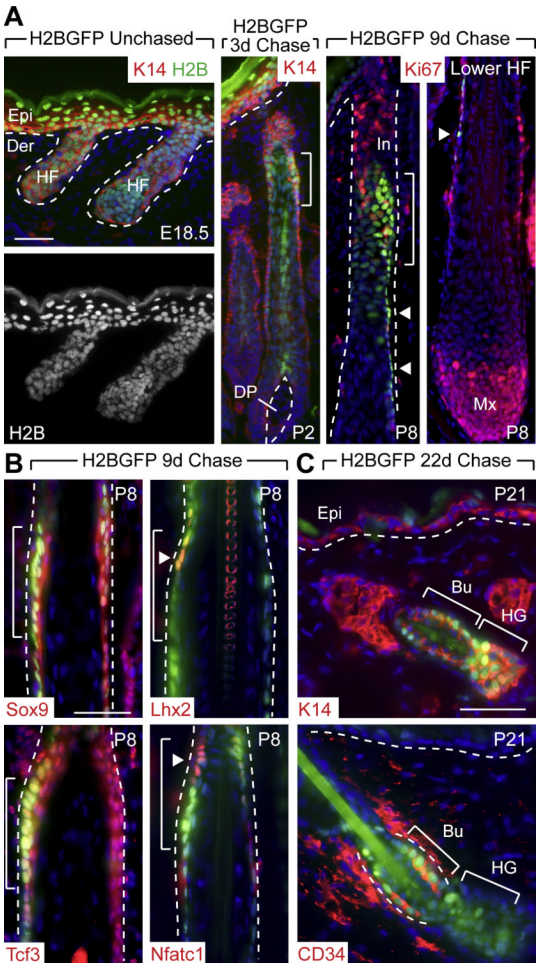

Figure 1. A Label Retaining Cell (LRC) Population Expressing SC Markers is Specified Early in HF Morphogenesis and Gives Rise to the Adult Bulge SC Niche

K5-tetVP16/TRE-H2BGFP double transgenic mice were chased at E18.5 to shut off H2B-GFP expression and identify label retaining cells (LRCs) within the early postnatal skin epithelium (P2-P8). **(A)** Appearance of LRCs during HF morphogenesis. Shown are representative skin sections with green H2B-GFP epifluorescence and counterlabeling with indicated antibodies (Abs) (red). After 3d of chase, the brightest H2B-GFP LRCs in the HF reside in a narrow zone of the upper ORS (brackets in 1A-1B) and are distinct from rapidly proliferating (Ki67-positive) cells, abundant in the infundibulum (In) and matrix (Mx). Arrowheads indicate a trail of slightly dimmer H2B-GFP LRCs extending down the ORS. Dotted lines denote the basement membrane that separates the interfollicular epidermis (Epi) and HF from the underlying dermis (Der) and dermal papilla (DP). (**B**) Immunofluorescence reveals partial co-localization (brackets, arrowheads) of LRCs with Abs specific for transcription factors expressed preferentially in adult bulge cells. (**C**) Immunofluorescence shows that after 22d of chase, LRCs labeled during embryogenesis are found exclusively in the adult bulge (Bu) niche (CD34-positive) and secondary hair germ (HG), and not in the K5/K14-positive basal layer of the sebaceous gland or interfollicular epidermis (Epi). Scale bars, 50 μm.

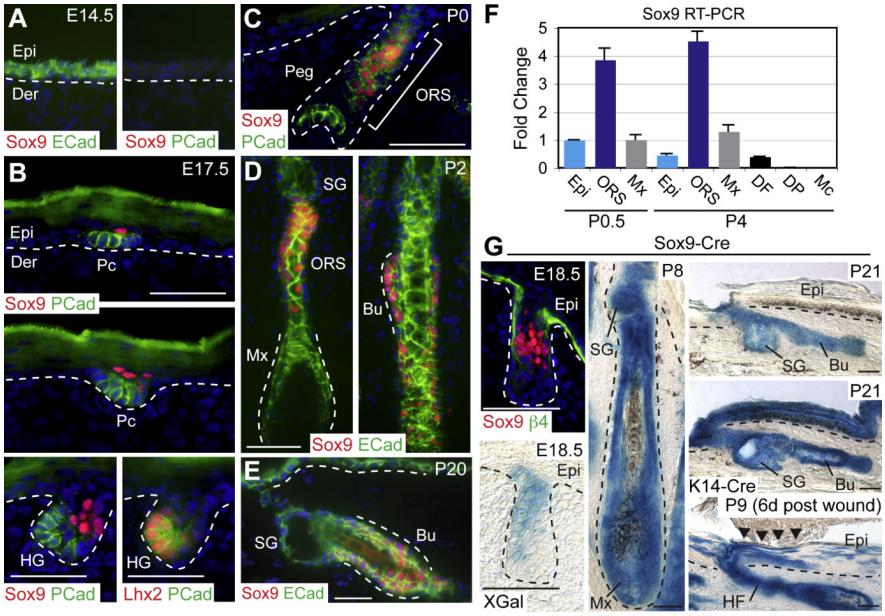

Figure 2. Sox9 is Expressed Early in Developing HFs, and Sox9-derived Progeny can Contribute to all Skin Epithelial Lineages

(A-E) Immunofluorescence microscopy with indicated Abs (color coded). Sox9 is first expressed in a few suprabasal cells of the hair placode (Pc), while P-cadherin (Pcad) and Lhx2 mark basal Pc cells. As morphogenesis proceeds, Sox9 continues to mark a zone of cells within the upper ORS, a region that becomes the bulge of the adult follicle. Note that during the rapid anagen growth phase at P2, Sox9 expression is absent from the transit-amplifying matrix. Dotted lines indicate epidermal-dermal border. ECad, E-Cadherin. **(F)** Real time PCR of FACS-purified populations from the skin (Rendl et al., 2005) reveals the specificity of Sox9 mRNA expression in the ORS. DF, dermal fibroblasts; Mc, melanocytes. **(G)** Genetic marking studies with *Sox9-Cre/R26R* reporter mice. Blue XGal staining marks β-galactosidase activity, reflective of Sox9-expressing cells and their progeny in tail skin HFs. At E18.5, XGal staining is similar to Sox9 protein expression. By P8 and thereafter, the entire HF and SGs are nearly completely comprised of blue cells, indicating derivation exclusively from Sox9-expressing cells. *K14-Cre/R26R* skin provides a positive control for XGal reactivity in the IFE. Scratch wounding of *Sox9-Cre/R26R* P3 mice demonstrates the contribution of Sox9-derived HF cells to the IFE lineage. β4, β4-Integrin. Other abbreviations are as in the legend for Figure 1. Scale bars, 50 μm.

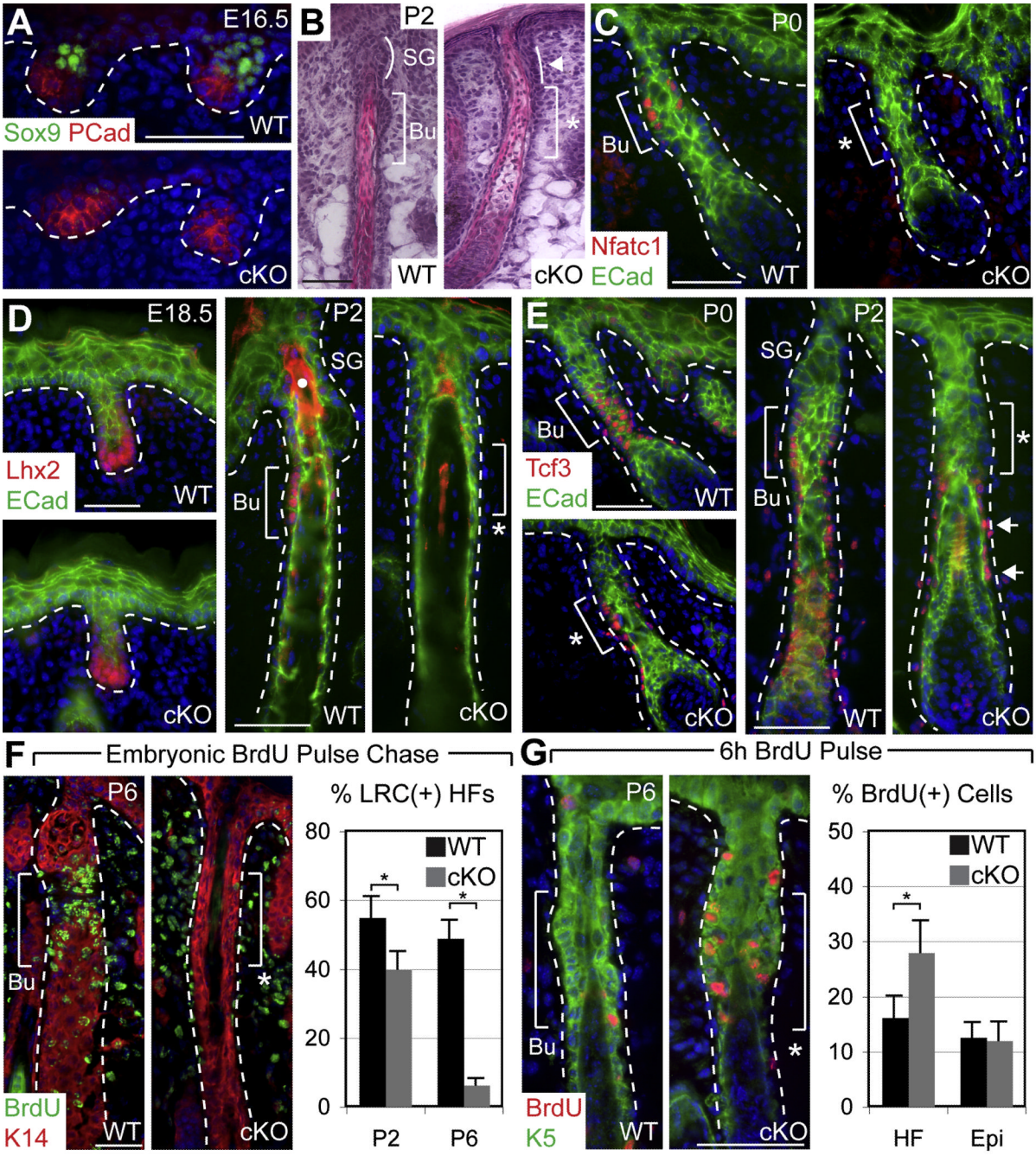

Figure 3. Failure of Quiescent Early Bulge SCs to Form when Sox9 is Conditionally Targeted in Embryonic Skin

WT early bulge region (Bu) and approximate cKO bulge region (asterisk) are indicated by brackets. White dotted lines denote epidermal-dermal border. Abs for immunofluorescence are color-coded. **(A)** Immunofluorescence of E16.5 backskin shows absence of Sox9 in cKO placodes and hair germs. **(B)** Hematoxylin & eosin stained P2 backskin reveals that the thickened zone of ORS which normally develops just below the SG (curved line) is absent in cKO HFs. **(C-E)** Immunofluorescence shows that Nfatc1 marking developing bulge cells never appears in cKO follicles. In contrast, Lhx2 is appropriately expressed at the leading edge of cKO follicles but is completely lost by P2. Tcf3, expressed in developing bulge cells

and lower ORS, is present in P0 cKO follicles, but is progressively lost, and at P2, Tcf3 is expressed only in the lower ORS. White dot in (D) marks autofluorescent hair shaft. **(F)** An E17-E18 embryonic BrdU pulse-chase demonstrates that early LRCs do not form in *Sox9* cKO HFs. Immunofluorescence shows discrete accumulation of BrdU(+) LRCs in the WT early bulge region and absence in cKO. After 7d of chase, an ~8X reduction in BrdU LRC(+) HFs is observed in cKO vs WT follicles. Graph shows percentages (± SEM). **(G)** A 6h BrdU pulse at P6 shows enhanced proliferation in the approximate bulge region of cKO HFs. Immunofluorescence shows BrdU incorporation in the ORS and graph indicates the percentage (± SEM) of cells in the ORS or IFE positive for BrdU incorporation. Asterisk indicates p-value < 0.05. Scale bars, 50 μm.

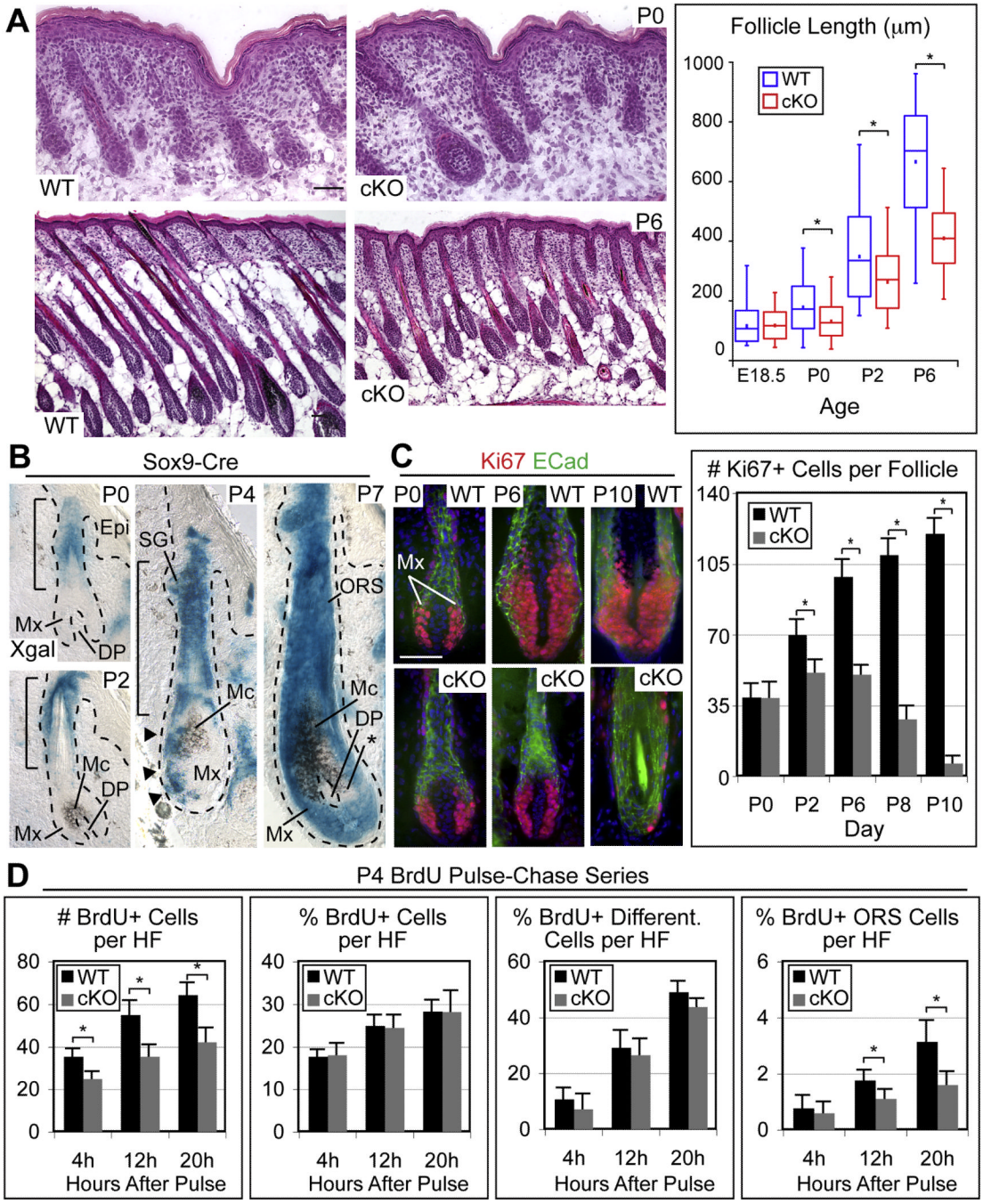

Figure 4. Early Bulge SCs are Required to Maintain a Transit-Amplifying Matrix Population

(A) H&E stained backskin reveals normal HF density but impaired HF growth. Box and whisker plots quantify HF length and reveal defects by P0: minimum and maximum length are marked by whiskers; upper and lower box boundaries indicate quartile divisions; central line indicates median; square dot indicates mean length. **(B)** Genetic marking studies with *Sox9-Cre/R26R* reporter mice. Blue XGal staining marks Sox9-expressing cells and their progeny, demonstrating a temporal progression of blue ORS cells that move to and enter the matrix (Mx), eventually replacing all prior Mx cells during HF morphogenesis. The mesenchymal DP encapsulated by the Mx and melanocytes (Mc) are not affected. However, Mc provide brown pigment to differentiating hair shaft cells, giving some intermingled blue

and brown cells. Asterisk indicates XGal negative Mx cells. **(C)** Immunofluorescent tracking of Ki67 positive Mx cells over time. The cKO Mx expands only transiently before reaching an abnormally small maximal size. After P2, the cKO Mx shrinks and ceases proliferation. Representative examples are shown. ECad, E-cadherin. Graph displays the average number of Ki67 positive cells (± SD) found in the Mx. **(D)** Mx proliferation and differentiation kinetics were analyzed by short BrdU pulse-chases at P4. Note that the percentage of BrdU positive cells in the lower ORS was lower in cKO HFs compared to WT at both the 12h and 20h timepoints, whereas the percentage of total BrdU positive cells and BrdU/AE13 double positive, differentiated cells was largely unchanged. Graphs indicate averages (± SEM). Asterisk indicates p-value < 0.05. Scale bars, 50 μm.

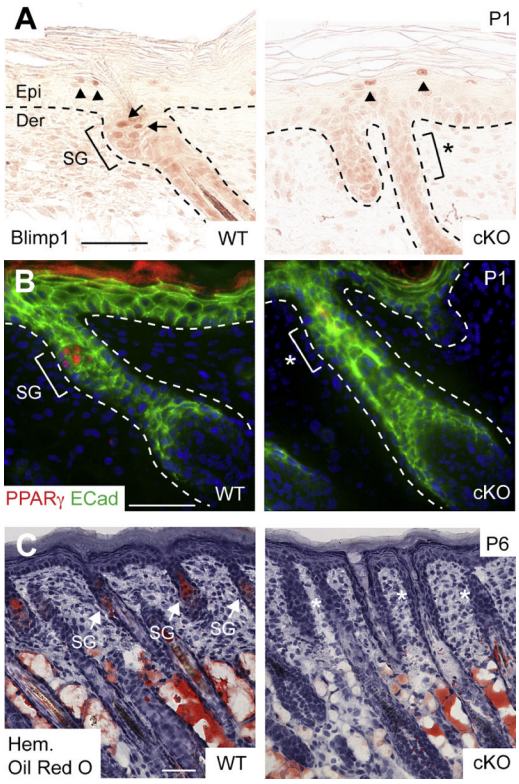

Figure 5. Early bulge SCs are Required to Form the Complete Pilosebaceous Unit

(A) Immunohistochemical analysis of Blimp1 expression shows an absence of unipotent SG progenitors in the upper ORS of *Sox9* cKO HFs where the SG should normally form. Arrows indicate Blimp1-positive cells in the early SG of a WT HF. Note that Blimp1 is still appropriately expressed in subrabasal cells of cKO epidermis (arrowheads). **(B)** Immunofluorescence reveals that PPARγ, a sebocyte differentiation marker (bracket, SG), is absent in cKO follicles (bracket, asterisk). **(C)** Detection of lipids by Oil-red O staining reveals no evidence of lipid-accumulating SGs (arrows) associated with cKO follicles (asterisks). By contrast, the formation of dermal fat is not affected when *Sox9* is conditionally targeted by *K14-Cre*. Hem, hematoxylin. Other abbreviations are as in the legend for Figure 1. Scale bars, 50 μm.

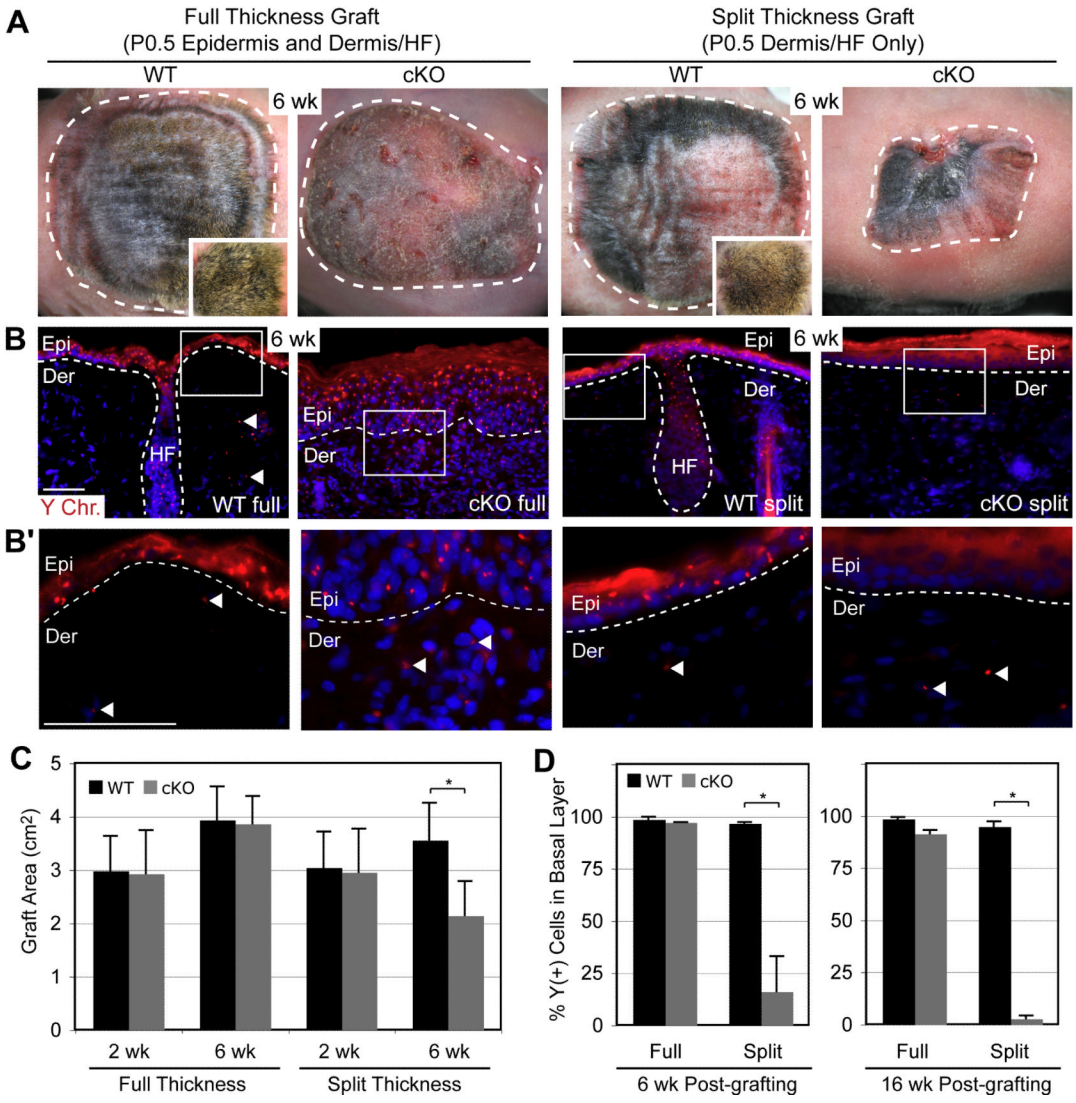

Figure 6. Early Bulge SCs are Required for HF-mediated Wound Repair of Interfollicular Epidermis

Full thickness (epidermis and dermis/HFs) and split thickness (dermis/HFs) skins from newborn male WT and *Sox9* cKO mice were grafted onto female *Nude* recipients and analyzed for their gross appearance 6 wks after placement (**A**) and contribution of engrafted cells to the repaired epithelium, as judged by Y-chromosome in situ hybridization (Y-FISH) (**B**). Quantifications of these data are presented in (**C**) and (**D**), respectively. Notes: 1) WT grafts were shaved to expose skin surface. Insets in (A) show unshaved hair coat. 2) Quantifications in (C) are of average graft areas (± SD) from 10 experiments. Full thickness WT and cKO grafts have a similar average area, while split thickness cKO grafts are smaller compared to split thickness WT grafts at 6wks. All grafts except cKO split thickness increased in area over time. 3) Y-FISH reveals that *Sox9* cKO HFs are impaired in contributing to the epidermis (Epi). 4) Full thickness grafts show abundant Y chromosome labeling, indicating donor origin and efficacy of the engraftments. 5) Split thickness grafts show a striking absence of Y-positive cells in cKO vs WT epidermis. Only *Nude*-derived, Y-negative cells exist in the re-epithelialized cKO epidermis. Panels in B' represent enlargements of boxed areas in (B) and illustrate Y-positive cells (arrowheads) in the dermis of all grafts. Dotted white lines indicate epidermal-dermal border. Graph indicates the

average %Y-positive cells in the basal layer (± SD). Asterisk indicates statistical significance of $p < 0.01$. Scale bars, 50 μm.

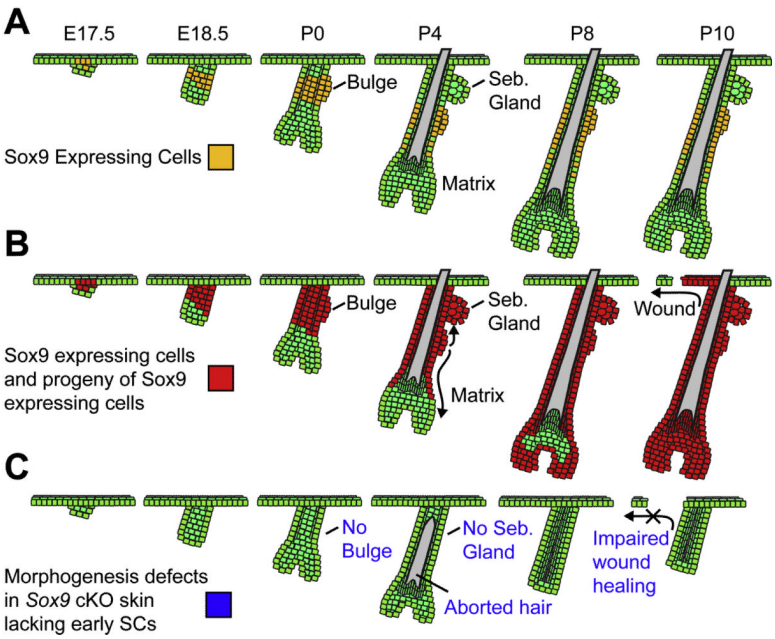

Figure 7. Model Depicting Roles for Sox9 during Embryonic and Early Postnatal Skin Development

(A) Sox9 expression begins in the hair placode, where it marks a few suprabasal cells overlying PCad/Lhx2-positive basal cells at the leading edge. It persists in the upper ORS, where it overlaps with the quiescent LRCs that give rise to the adult bulge. **(B)** Genetic marking is consistent with the notion that Sox9 labels presumptive bulge stem cells within the upper ORS of the developing HF. As HF morphogenesis proceeds, Sox9-expressing cells give rise to the ORS that extends below the early bulge and also the emerging SG above the early bulge. Subsequently, Sox9-expressing cells move down the ORS and completely replace the initial matrix, which is likely to be derived from the Lhx2-positive basal cells of the placode. Upon completion of morphogenesis, the entire HF is composed of Sox9-expressing cells and their progeny. In the presence of a wound stimulus, the progeny of Sox9-expressing cells can robustly contribute to IFE repair. **(C)** Conditional ablation of *Sox9* prior to HF morphogenesis reveals that in the absence of Sox9, an early bulge SC population never forms, and all three epithelial lineages are affected. HF differentiation is initially unimpaired, but a lack of SC input to replenish transit-amplifying matrix cells results in aborted hair production. The sebaceous gland never forms in the absence of SCs, and HF contribution to wounded IFE is markedly impaired.